Available online at www.sciencedirect.com

ScienceDirect

Ceramics International 41 (2015) 1361–1365

CERAMICS INTERNATIONAL

www.elsevier.com/locate/ceramint

Strength development, bioactivity and biodegradability of forsterite nanostructure scaffold

Seyed Mehdi Mirhadi*, Amir Abbas Nourbakhsh, Najmeh Lotfian, Behnam Hosseini

Department of Materials Engineering, Shahreza Branch, Islamic Azad University, 86145-311 Shahreza, Isfahan, Iran

Received 5 September 2014; received in revised form 10 September 2014; accepted 11 September 2014
Available online 19 September 2014

Abstract

Highly porous forsterite nanostructure scaffolds with high compressive strength were prepared by a two steps sintering method. It was found that the formation of enstatite glassy phase during heat treatment at high temperature is responsible for the strengthening mechanism of the prepared scaffolds. The in vitro bioactivity and degradability of the scaffolds were also determined by immersing them in simulated body fluid (SBF) and Ringer's solution, respectively. The results demonstrated that nanostructure scaffolds with the mean crystallite size of about 33 nm showed suitable bioactivity. Also it was found that the prepared nanostructure scaffolds have a good biodegradability and can release magnesium ions into Ringer's solution. The formation of a small amount of glassy phase (enstatite), which improved the compressive strength of the prepared scaffolds, did not have a detrimental influence on the bioactivity and biodegradability of the forsterite structure in vitro.
© 2014 Elsevier Ltd and Techna Group S.r.l. All rights reserved.

Keywords: Forsterite; Biodegradability; Nanomaterials; Scaffolds

1. Introduction

Fabrication of scaffolds with high porosity, similar to the spongy bone of human body, and with high compressive strength is one of the aims of many scientists in tissue engineering [1,2]. Hydroxyapatite is one of the most important bioceramics due to its high bioactivity and osteoconductivity properties. However, the orthopedic applications of hydroxyapatite ceramics have been limited as a result of the low fracture toughness and inappropriate mechanical properties [3,4].

Recently, forsterite has been proposed as a new bioceramic for tissue engineering application [5–9]. It has been proved that nanostructure forsterite has bioactive properties and can form apatite layer on its surface [5,7]. On the other hand, nanostructure forsterite can release magnesium and silicon ions into the biological medium and show good biodegradability [7]. It has been shown that the bioactivity and biodegradability of forsterite ceramics depend on the crystallinity of forsterite structure; with increasing crystallinity the bioactivity and biodegradability of forsterite structure decreased [7].

In our previous paper [10], we synthesized nanostructure forsterite scaffolds with high porosity and high compressive strength almost similar to spongy bone in human body. In the present paper, the mechanism behind the increased strength is studied. Also the bioactivity and biodegradability of the obtained scaffolds were investigated to evaluate the influence of enstatite on the bio-behavior. The obtained results can open a promising approach to utilize forsterite nanostructure scaffolds for load bearing application in tissue engineering.

2. Experimental procedure

Forsterite nanostructure scaffolds were synthesized according to our previous study [10]. First, forsterite powder was synthesized from talc and $MgCO_3$ powders [11]. A slurry of forsterite and ethyl alcohol was prepared and pre-cut sponges were soaked in the slurry. The saturated sponges were then sintered at different temperatures for various holding times [10]. Table 1 shows the heat treatment regimes. To clarify the

*Corresponding author. Tel.: +98 31 53292201; fax: +98 31 53502701.
E-mail address: Mirhadi@iaush.ac.ir (S. Mehdi Mirhadi).

http://dx.doi.org/10.1016/j.ceramint.2014.09.069
0272-8842/© 2014 Elsevier Ltd and Techna Group S.r.l. All rights reserved.

Table 1
designation, heat treatment regimes, porosity and compressive strength of prepared forsterite scaffolds [10].

Designation	Sample A	Sample B	Sample C	Sample D
Heat treatment				
Step 1	HR = 2 °C/min	HR = 2 °C/min	HR = 2 °C/min	HR = 2 °C/min
	T = 300 °C	T = 300 °C	T = 300 °C	T = 300 °C
Step 2	HR = 5 °C/min	HR = 5 °C/min	HR = 5 °C/min	HR = 5 °C/min
	T = 1300 °C	T = 1300 °C	T = 1500 °C	T = 1500 °C
Step 3	T = 1300 °C	T = 1300 °C	T = 1500 °C	T = 1500 °C
	HT = 5 min	HT = 60 min	HT = 60 min	HT = 60 min
Step 4	CR = 50 °C/min	CR = 50 °C/min	CR = 50 °C/min	CR = 50 °C/min
	T = 800 °C	T = 800 °C	T = 800 °C	T = 800 °C
Step 5	T = 800 °C	T = 800 °C	T = 800 °C	T = 800 °C
	HT = 300 min	HT = 900 min	HT = 300 min	HT = 900 min
Step 6	CR = 5 °C/min	CR = 5 °C/min	CR = 5 °C/min	CR = 5 °C/min
	T = 25 °C	T = 25 °C	T = 25 °C	T = 25 °C
Porosity (%)	86	83	80	86
Compressive strength (Mpa)	0.34 ($\pm$0.02)	0.22 ($\pm$0.05)	4.33 ($\pm$0.02)	3.49 ($\pm$0.02)

HR = heating rate, CR = cooling rate and HT = holding time.

designations, for example, the heat treatment regime of sample A is as follows: the sample was heated to 300 °C at the heating rate of 2 °C/min. Then the temperature was increased to 1300 °C at the heating rate of 5 °C/min. At 1300 °C, the specimen is kept for 5 min and then it is cooled down to 800 °C at the cooling rate of 50 °C/min. Subsequently it is kept at 800 °C for 300 min holding time and finally it is cooled down to 25 °C at the cooling rate of 5 °C/min. For this study, we choose 4 different heating regimes based on the lowest and highest compressive strength obtained in our previous study [10].

In vitro bioactivity of the obtained scaffolds was investigated by soaking the prepared samples in the SBF for 1, 2, 4, 7, 14, 21, and 28 days. For this purpose, the prepared scaffolds were soaked in 100 ml SBF without refreshing the soaking medium. This procedure has been widely used to prove the similarity between in vitro and in vivo behavior of certain bioceramic composites. The SBF was prepared according to the standard procedure described by Kokubo and Takadama [12]. The soaking experiment was performed in a shaking bath maintained at 37 °C. After soaking, the samples were gently rinsed with deionized water to remove SBF solutions followed by drying at 100 °C for 24 h. To evaluate the degradation rate, the prepared scaffolds were soaked in 100 ml Ringer's solution (pH 7.40) at 37 °C in a shaking water bath for 1, 2, 4, 7, 14, 21, and 28 days without refreshing the soaking medium. After soaking the samples were dried at 100 °C for 1 day, and the final weight of each sample was accurately measured. The weight loss was expressed as a percentage of the initial weight.

A Philips X'PERT MPD diffractometer with Cu Kα radiation (λ = 0.154056 nm) was used for X-ray diffractometry (XRD) analysis to determine the structure of the obtained scaffolds. XRD patterns were recorded in the 2θ range of 20–80° (a step size of 0.04° and a time per step of 1 s). The transmission electron microscopy (TEM; Leo 912AB) technique was utilized to characterize the morphology and nanostructure of the synthesized scaffolds. The apatite formation on the surface of the samples as a consequence of the precipitation process of calcium phosphate was investigated by Fourier transitioned-infrared spectroscopy (FTIR; Bomem, MB 100), scanning electron microscopy (SEM; Seron, AIS2100), and energy dispersive X-ray (EDX). The concentrations of Ca and Mg ions of the SBF and Ringer's solutions after soaking were determined by an atomic absorption spectrometer (AAS; Perkin Elmer, 2380), and the changes in pH of soaking solutions were also measured at predetermined time intervals (0–28 days) using an electrolyte-type pH meter.

3. Results and discussions

Fig. 1 shows the XRD traces of the prepared scaffolds after different heat treatment regimes. As can be seen, forsterite (XRD JCPDS data file no. 34-0189) was the dominant phase in all the XRD patterns. On the other hand, traces of enstatite (XRD JCPDS data file no. 11-0273) were also observed in the XRD traces. As we showed in our previous study [10], the scaffolds were prepared from single-phase forsterite powder. However after various heat treatment regimes, a very small amount of metastable enstatite can be observed in the XRD patterns. The reappearance of enstatite is reported in previous studies due to its faster kinetics [13–15]. This phase appeared to be stable up to 1600 °C [16]. With the formation of enstatite in the form of glassy phase, new bonds and better attachments were provided between forsterite grains and hence the compressive strength of the scaffolds increased.

By increasing the sintering temperature or holding time, the intensity of XRD peaks increased while their width decreased due to the increase in the grain size with higher degree of crystallinity. It should be noticed that with increasing sintering temperature the compressive strength of the scaffolds increases due to the formation of higher amount of enstatite and better sintering of the structure but this may affect adversely on the bioactivity and biodegradability of the formed scaffolds [7].

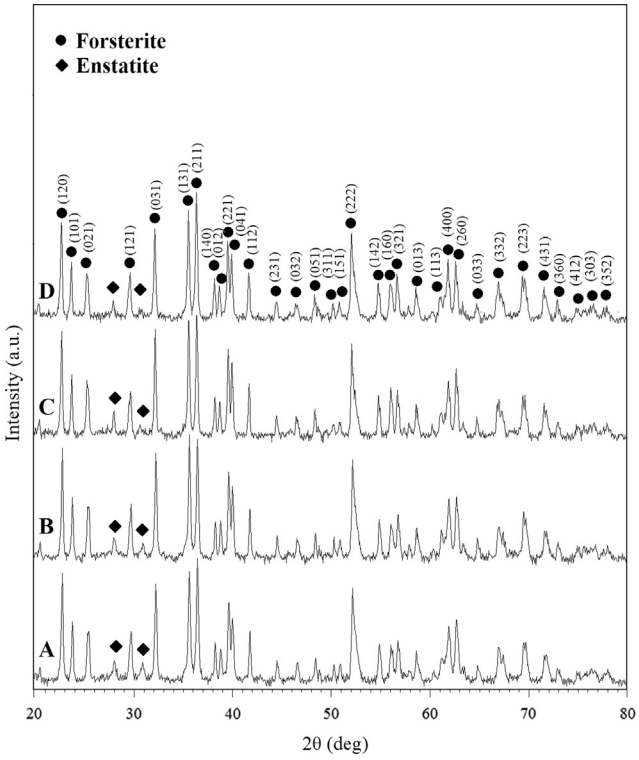

Fig. 1. XRD patterns of various scaffolds heat treated at different temperatures.

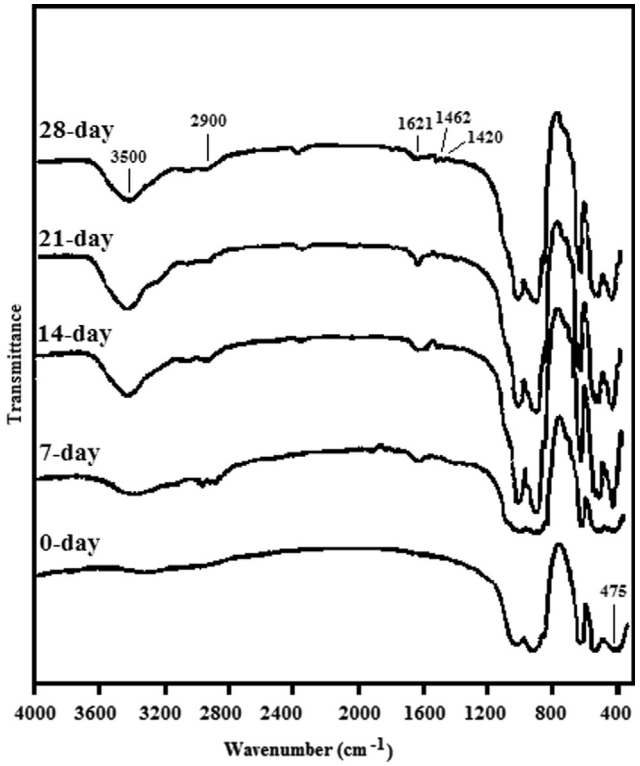

Fig. 3. FTIR spectra of sample D before and after soaking in SBF for various periods of time.

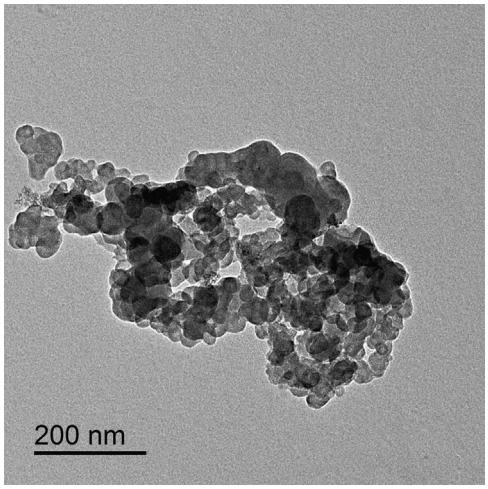

Fig. 2. TEM micrograph of powders obtained from sample D.

The TEM micrograph of sample D is shown in Fig. 2. As can be seen, the grains are in the range of 18–78 nm with the mean of 33 nm and the standard deviation of 11 nm. Sample D has the longest holding time at high temperatures. Other specimens had smaller grain size. Therefore for further study we investigate the bioactivity and biodegradability of sample D.

In order to determine the bioactivity of the specimens, prepared scaffolds were soaked in SBF for various days. Fig. 3 shows the infrared spectra of sample D after soaking in SBF for various periods of time. As can be seen, infrared spectra of sample D before immersion in SBF corresponded to the characteristic bands of enstatite and forsterite. The bands related to the characteristic bands of enstatite and forsterite appeared in the range of 1100–800 cm^{-1} (SiO_4 stretching), 650–500 cm^{-1} (SiO_4 bending), and at 475 cm^{-1} (MgO_6 modes). These results prove the formation of enstatite and forsterite as shown in the XRD patterns (Fig. 1). The obtained peaks agreed with the results reported in previous studies [5]. By immersing the specimens in the SBF, new absorption bands related to O–H, C–O, and P–O were observed. The bands at 3500 and 1621 cm^{-1} belonged to hydroxyl groups in the hydroxyapatite. Those bands at 1462 and 1420 cm^{-1} fit with bands of apatite structure carbonate groups [17]. The low intense bands noticed at about 2900 cm^{-1} may be attributed to H–C–O functional groups [18]. Furthermore, bands related to phosphate groups were situated in the range of 1100–1000 and 600–550 cm^{-1}. These three bands are the characteristic bands of apatite crystals which suggest the formation of apatite on the surface layer of forsterite samples after soaking in SBF [19]. As can be seen, with increasing soaking time the intensity of O–H, C–O, and P–O absorption bands gradually increased as a result of formation of higher amount of hydroxy-carbonate apatite (HCA) on the surface of forsterite samples [17]. The immersion test in SBF and formation of amorphous HCA precipitation on the surface of materials could be regarded as the prevalent test in order to determine the bioactivity of materials [18].

The AAS analysis was performed in order to determine the concentration of Mg, P and Ca ions in the SBF solution. Fig. 4 shows the results of AAS analysis obtained from SBF solutions

of sample D after different soaking times. Also, pH changes of solutions in the time span are shown. In general, increasing the pH and Mg ions and decreasing the Ca and P ions concentration in the SBF were the overall consequence of soaking the scaffolds samples. As can be seen in Fig. 4, most concentration changes of ions and pH of the SBF were in the first day of soaking as Mg ions concentration increased from 17 to 21 ppm, Ca and P ions concentration decreased from 112 to 96 ppm and 52 to 35 ppm, respectively. Also the pH of the solution increased from 7.4 to 7.54. These results revealed the release of Mg ions from the scaffolds ceramics accompanied with the deposition of Ca and P ions on the surface of the scaffolds. On increasing the soaking time in the SBF, the Ca and P ions concentration decreased at a lower rate, which could be ascribed to the consumption of these ions and the formation of apatite on the surface of forsterite samples. On the other hand, the slope of the Mg ions concentration decreased with increasing soaking time which can be due to the saturation of SBF solution from Mg ions.

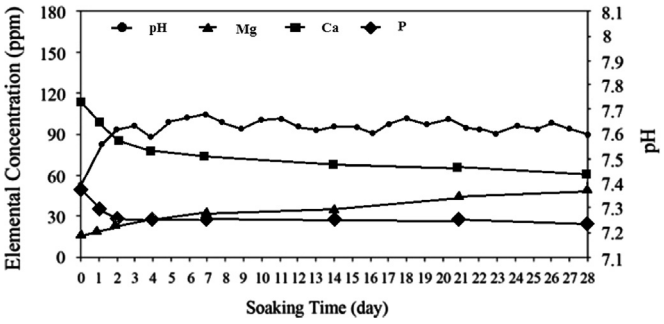

Fig. 4. Changes of Ca, P and Mg ions concentrations, and pH of the SBF of sample D after soaking for various periods of time.

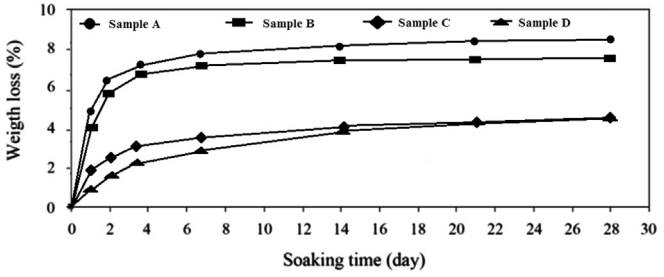

Fig. 5. The weight loss of various scaffolds soaked in Ringer's solution after different periods of time.

In order to determine the degradation rate, scaffolds were immersed in Ringer's solution at 37 °C up to 4 weeks. The weight loss of various scaffolds is shown in Fig. 5. As can be seen, sample A had the maximum weight loss while sample D had the minimum one. The degradation rate of the scaffolds decreased with increasing sintering temperature due to the increase in the crystallinity [7]. Also it was found that enstatite had negligible influence on the degradation rate of the scaffolds.

Fig. 6a and b shows the SEM results of sample D before and after immersing in SBF for 28 days. As can be seen, after soaking for 28 days some pores are filled with Ca–P precipitations. The EDX spectra proved the presence of calcium and phosphorus in this specimen. Considering the results of FTIR patterns and changes of the ions concentration in the SBF, it is expected that the formed deposits were hydroxy-carbonate apatite.

4. Conclusion

The strengthening mechanism of forsterite scaffolds was investigated. It was found that the formation of glassy enstatite is responsible for increasing the compressive strength of the scaffolds at high temperatures. The bioactivity of nanostructure scaffolds was studied in SBF to evaluate the in vitro behavior of the prepared specimens. Furthermore, Ringer's solution was used to determine the degradation rate of nanostructure scaffolds. AAS, FTIR and EDS results showed the presence of hydroxycarbonate apatite on the surface of nanostructure scaffolds.

On the other hand, it was found that the formation of enstatite has minimal influence on the degradation rate of the scaffolds. In summary, nanostructure forsterite scaffolds showed good compressive strength, bioactivity and biodegradability and could be a suitable candidate for hard tissue engineering in load bearing applications.

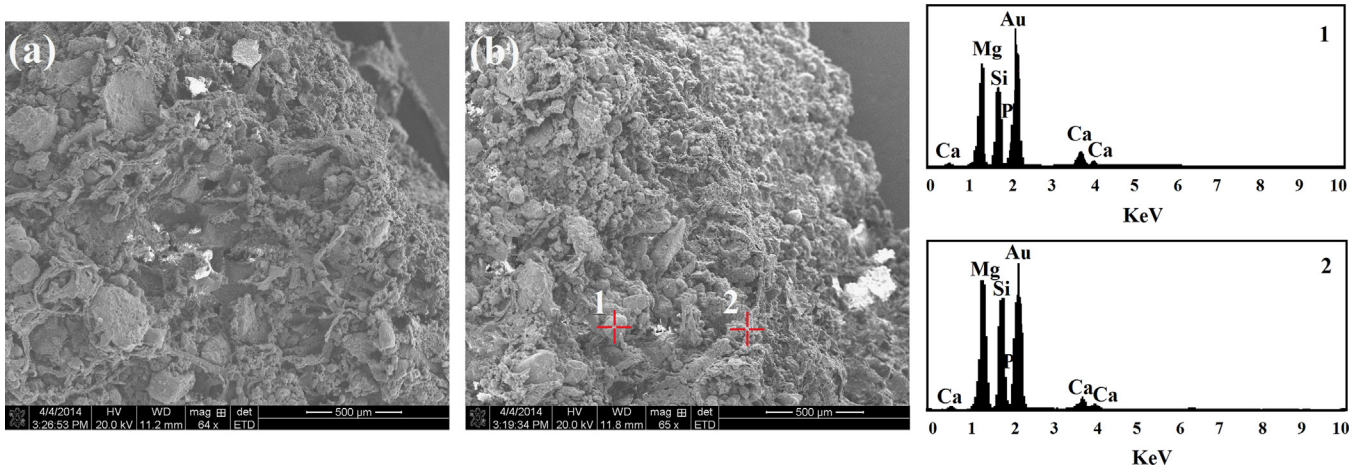

Fig. 6. SEM micrographs of the surfaces of nanostructure forsterite scaffolds (a) before and (b) after immersion in SBF for 28 days.

Acknowledgments

The authors thanks members of the Materials Science Laboratory of the Islamic Azad University of Shahreza for their helpful contributions to this work.

References

[1] S.I.R. Esfahani, F. Tavangarian, R. Emadi, Nanostructured bioactive glass coating on porous hydroxyapatite scaffold for strength enhancement, Mater. Lett. 62 (2008) 3428–3430.
[2] R. Emadi, S.I.R. Esfahani, F. Tavangarian, A novel, low temperature method for the preparation of ß-TCP/HAP biphasic nanostructured ceramic scaffold from natural cancellous bone, Mater. Lett. 64 (2010) 993–996.
[3] M.V. Regi, J.M.G. Calbet, Calcium phosphate as substitution of bone tissues, Prog. Solid State Chem. 32 (2004) 1–31.
[4] W. Suchanek, M. Yoshimura, Processing and properties of hydroxyapatite-based biomaterials for use as hard tissue replacement implants, J. Mater. Res. 13 (1998) 94–117.
[5] F. Tavangarian, R. Emadi, Nanostructure effects on the bioactivity of forsterite bioceramic, Mater. Lett. 65 (2011) 740–743.
[6] R. Emadi, F. Tavangarian, S.R.I. Esfahani, A. Sheikhhosseini, M. Kharaziha, Nanostructured forsterite coating strengthens porous hydroxyapatite for bone tissue engineering, J. Am. Ceram. Soc. 93 (2010) 2679–2683.
[7] F. Tavangarian, R. Emadi, Improving degradation rate and apatite formation ability of nanostructure forsterite, Ceram. Int. 37 (2011) 2275–2280.
[8] F. Tavangarian, R. Emadi, Effects of mechanical activation and chlorine ion on nanoparticle forsterite formation, Mater. Lett. 65 (2011) 126–129.
[9] F. Tavangarian, R. Emadi, A. Shafyei, Influence of mechanical activation and thermal treatment time on nanoparticle forsterite formation mechanism, Powder Technol. 198 (2010) 412–416.
[10] S.M. Mirhadi, Synthesis and characterization of nanostructured forsterite scaffolds using two step sintering method, J. Alloys Compd 610 (2014) 399–401.
[11] F. Tavangarian, R. Emadi, Mechanical activation assisted synthesis of pure nanocrystalline forsterite powder, J. Alloys Compd 485 (2009) 648–652.
[12] T. Kokubo, H. Takadama, How useful is SBF in predicting in vivo bone bioactivity?, Biomaterials 27 (2006) 2907–2915
[13] F. Tavangarian, R. Emadi, Effects of fluorine ion and mechanical activation on nanostructure forsterite formation mechanism, Powder Technol. 203 (2010) 180–186.
[14] R. Emadi, F. Tavangarian, Mechanochemical synthesis of single phase nanocrystalline forsterite powder, Int. J. Mod. Phys. B 24 (2010) 343–350.
[15] S.M. Mirhadi, F. Tavangarian, R. Emadi, Synthesis, characterization and formation mechanism of single-phase nanostructure bredigite powder, Mater. Sci. Eng. C 32 (2012) 133–139.
[16] A. Kazakos, S. Komarneri, R. Roy, Preparation and densification of forsterite (Mg_2SiO_4) by nanocomposite sol–gel processing, Mater. Lett. 10 (1990) 405–409.
[17] Y.L. Zhang, M. Mizuno, M. Yanagisawa, H. Takadama, Bioactive behaviors of porous apatite- and wollastonite-containing glass-ceramic in two kinds of simulated body fluid, J. Mater. Res. 18 (2003) 433–441.
[18] R. Murugan, S. Ramakrishna, K. Panduranga Rao, Nanoporous hydroxycarbonate apatite scaffold made of natural bone, Mater. Lett. 60 (2006) 2844–2847.
[19] B.O. Fowler, Vibrational assignments for calcium, strontium, and barium hydroxyapatite utilizing isotopic substitution, Inorg. Chem. 13 (1974) 194–207.